A Novel Potentially Toxic Cyanobacterial Species From the Genus Desmonostoc, Desmonostoc Alborizicum sp. nov., Iisolated From a Water Supply System of IranA

Bahareh Nowruzi (bahare77biol@yahoo.com)
Islamic Azad University https://orcid.org/0000-0001-6656-777X
Itzel Becerra-Absalón
Mexico National Cancer Institute: Instituto Nacional de Cancerologia

Research Article

Keywords: benthic habitats, ITS, Cyanobacteria, Nostocales, 16S rRNA gene phylogeny, polyphasic approach, qanat water system

Posted Date: March 8th, 2022

DOI: https://doi.org/10.21203/rs.3.rs-1404975/v1

Abstract

A cyanobacterial mat colonizing the wall of a qanat was found to be responsible for damages affecting the passage of water through the water supply system in Golestan province, Gorgan city, Iran. A qanat or kariz is a slightly sloping underground aqueduct used to transport water from water wells or aquifers to the surface for irrigation and drinking supply. A cyanobacterial strain was isolated from the mat and grown in BG11 liquid medium. Fragments of 16S rRNA, *mcy*G and *mcy*D genes were amplified and sequenced, as well as the 16S-23S internal transcribed spacer (ITS), from which secondary structures were analyzed. The obtained molecular data, together with morphological and physiological observations, were used to describe the new organism. The isolate was related to a morphotype of *Nostoc* sensu lato group, with similar characteristics of *Desmonostoc*, after microscopic inspections. The 16S rRNA phylogenetic analysis placed the isolate into the typical cluster of the recently proposed genus *Desmonostoc*. Morphological analysis revealed distinctive characteristic and secondary structures of 16S–23S rRNA (D1-D1´ and Box-B regions) derived from comparative analysis, which did not match known species of *Desmonostoc*. These results lead us to propose a novel *Desmonostoc* species, *Desmonostoc alborizicum*, which was described and compared with similar taxa. Furthermore, for the first time a potential toxic species of *Desmonostoc* was isolated from water supply, since the *mcy*D and *mcy*G genes of microcystin synthetase (*mcy*) cluster was successfully sequenced. The presence of the microcystin was confirmed by chemical analyses that also lead to the discovery of numerous other cyanobacterial secondary metabolites. We recognized substantial amounts of the potent microcystin variant microcystin-LR present in cell extracts of the *Desmonostoc* strain. Our findings contribute to a deeper understanding of diversity, systematics, and occurrence of *Desmonostoc* genus.

Introduction

Cyanobacteria are gram-negative bacteria with a long evolutionary history, and the only prokaryotic organisms capable of performing oxygenic photosynthesis [1]. Some of them are important to the nitrogen cycle, since they can fix atmospheric nitrogen. In addition to a high morphological diversity within this group of microorganisms, the chemical diversity of natural products that they are able to produce [2] allow them to survive in a range of highly competitive ecological niches [3].

The systematics of the phylum Cyanobacteria is challenging and has undergone several revisions during years [4, 5]. Moreover, some morphological characters may vary considerably in response to different environmental conditions, making species delimitation difficult if only based on morphological criteria.

The cyanobacterial genus *Nostoc* is a polyphyletic group according to molecular phylogeny, and the *Nostoc* sensu lato group has recently split into novel genera such as *Mojavia*, *Desmonostoc*, *Halotia* and *Aliinostoc* [6–9, respectively]. Morphologically, members of *Desmonostoc* form long vegetative filaments embedded in diffluent mucilaginous envelopes. Except for primordial stages, they never possess a tight periderm, and the filaments are never densely coiled with compact trichomes as found in *Nostoc* [7]. Further, elliptical akinetes are differentiated apoheterocytically in long chains, and both terminal and intercalary heterocytes are observed [7]. Phylogenetically, *Desmonostoc* comprises a coherent group separated from members of related taxa such as *Nostoc*, *Halotia* and *Mojavia* [7, 10]. *Desmonostoc* representatives can be usually found in non-extreme environments (*e.g.*, in moist or wet meadow, field and forest soils), and rarely in periphyton, biofilms as well as in deserts [7, 10]. To date, ten *Desmonostoc* species are known: *D. muscorum, D. entophytum* and *D. linckia* [7], *D. geniculatum* and *D. vinosum* [11], *D. salinum* [10], *D. punense* and *D. magnisporum* [12], *D. danxiaense* [13], and *D. persicum* [14]. However, *Desmonostoc* capability of cyanotoxin production has not been reported [10].

In addition to the 16S rRNA gene and phylogeny, the 16S–23S rRNA ITS secondary structures have largely been used to provide taxonomic resolution of novel cyanobacteria species [10, 15–20].

Mass occurrences of cyanotoxins are not only a significant problem in terms of water quality, but also pose a severe risk to human and animal health. They may contain potent hepato- and neurotoxic, as well as derma- and cytotoxic agents produced by strains of several cyanobacterial genera. Numerous cases of fatal animal poisonings, attributed to these toxins, have been reported around the globe over the past decades [21–23]. In freshwaters, blooms containing hepatotoxic agents are more frequent than those containing neurotoxins [24].

In October 2018, some kids were found suffering after drinking water from qanat in Golestan province, Gorgan city. The cyanobacterial isolate characterized in the present study was described morphologically, and analysed phylogenetically based on the 16S rRNA gene sequence coupled with its 16S–23S ITS secondary structures. Additional molecular markers (*mcy*G and *mcy*D genes) were also sequenced, analyzed and confirmed by chemical analyses. In addition to ecological information, morphological and molecular data allowed the proposal of a novel *Desmonostoc* species, *Desmonostoc alborizicum* sp. nov., colonizing the wall of a qanat in Iran as a

contribution to a better understanding of *Desmonostoc* diversity, systematics, and occurrence. Further, this is the first evidence of a potentially toxin-producing *Desmonostoc* due to the presence of the microcystin synthetase (*mcy*D and *mcy*G) gene.

Materials And Methods

Field surveys

The cyanobacterial mat was collected in October 2018 from a qanat fresh water system, latitude (36°51′25″N) and longitude (54°26′55″E), in Golestan province, Gorgan city, Iran. Fresh environmental samples were collected from the surface of qanat walls using a sterilized knife, which were placed into cone-shaped plastic bottles (Falcon® conical tubes), and transported to the laboratory for the subsequent isolation and identification. The sampling was done only from the surface of qanat walls exposed to light intensity over the water level that favored the mat density.

Physicochemical parameters: - Physical and chemical parameters such as temperature (°C) and pH of water were recorded at the sampling time. Conductivity (mS/cm) was measured according to McCleskey *et al.* method [25], and dissolved oxygen (ppm) following Singh *et al.* [26]. Phosphate and nitrate were quantified spectrophotometrically according to Sa'id and Mahmud method [27].

Cyanobacterial isolation and morphological evaluation: In the laboratory, small pieces of the cyanobacterial mat were spread into 1.2%-agar-solidified BG-11_0 medium [28] and cultivated. The biomass was constantly analyzed under a microscope and successive streaking was performed until a unicyanobacterial colony was obtained. The isolate was temporarily named 1387 and maintained in a 250 mL cotton-stoppered Erlenmeyer flask containing liquid BG-11_0 medium at 28 ± 2 ºC with periodic shaking (twice a day), illumination of ca. 50–55 µmoL photons $m^{-2}s^{-1}$, and a regime of 14:10 h light: dark cycle. Morphological observations were made using an Olympus CX31RTS5 (Olympus, Tokyo, Japan) stereoscope equipped with a QImaging GO-3 digital camera (Teledyne QIMAGING, Surrey, British Columbia, Canada) and an Olympus BX43 microscope equipped with manufactured Sc50 digital camera (Olympus, Tokyo, Japan). Cell parameters were measured using the DP–SOFT software; 50 to 200 measurements were taken for each parameter to describe the trait variability. Identification of the isolate was carried out according to Komárek *et al.* [4]. In addition, recent studies dealing with the description of new *Desmonostoc* species were considered [7, 10–12, 14]. A unialgal culture was deposited in the Cyanobacteria Culture Collection (CCC) and dry type material into ALBORZ herbarium. Both culture collection and herbarium are affiliated to the Science and Research Branch of the Islamic Azad University, Tehran, Iran.

Exsiccated and fresh cultures were deposited at the Cyanobacteria Culture Collection (CCC) and the ALBORZ Herbarium, at the Science and Research Branch, Islamic Azad University, Tehran, with the accession numbers CCC1387-a and CCC1387-b, respectively. A reference strain (MCC 5190) was deposited at the National Centre for Microbial Resource (NCMR), India.

Pcr Amplification Of 16s Rrna Gene And 16s ± 23s Internal Transcribed Spacer (Its)

Genomic DNA was extracted from a 16-day-old log phase culture using the HiPurA™ Bacterial Genomic DNA Purification Kit MB505 (HiMedia Lab, Mumbai, India), following the manufacturer's instructions, except for an increase of incubation time with lysis solutions AL and C1, which was set at 60 and 20 min, respectively.

Amplification of 16S rRNA gene comprised of one forward primer and a reverse primer [29–30] were used for complete amplification of 16S rRNA gene. One PCR reaction was comprised of 1 time buffer solution (DyNAzyme PCR buffer; Finnzymes, Espoo, Finland), 0.5 µm forward primer, 0.5 µm reverse primer and 0.5 U Taq polymerase as well as 1 µL template DNA and sterile water in a total volume of 20 µL. The template DNA concentration of the studied strains in the reaction accounted for approximately 140 ng. The amplification reactions were conducted in a thermocycler (iCycler; Bio-Rad, Foster City, CA, USA) with the program at table S1.

Internal spacer (ITS) was amplified with primer primers ITSF and ITSR. Moreover, eighteen internal oligonucleotide primers comprised of one forward primer and a reverse primer were used for complete amplification of 16S rRNA gene (Table S2).

Cloning was performed by using the TOPO Ta cloning system with the vector 2.1 –TOPO (Invitrogen, Carlsbad, USA) according to the manufacturer instructions. Ligation reactions were incubated for 30 minutes at room temperature and transformations were carried out using chemically competent TOPO10 *Eschericha Coli*- cells. The vector PCR 2.1 TOPO contains ampicillin and Kanamycin resistance genes and the Lac Z gene, which assisted in the detection and selection of clones with the desired insert. The *lacZ* gene codes for β-galactosidas enzyme which hydrolysis e.g. the compound 5-bromo-4-chloro-3-indolyl-β-D-galactopyranoside (X-gal) resulting in the release of blue colour. To find the correct clones, 40 µl of 50 mg ml^{-1} X-gal solution (promega, Madison, U.S. A.) was spread on Luria-

Bertani plates [31] containing 50 µg ml^{-1} of ampicilin (Sigma-Aldrich, Saint Louris, U.S.A) before plating the transformant cells. Insertion of foreign DNA into the *LacZ* gene during ligation disrupts and inactivates the gene and white colonies are obtained.

To screen microcystin synthetase gene cluster, the *mcy*D gene was selected as target molecule (Table S1). Reactions were made using 10–20 ng DNA template, 0.5 µM of each primer, 1.5 mM $MgCl_2$, 200 µM dNTPs, 1U/µL Taq DNA polymerase and ultrapure water to a 25-µL final volume in a thermal cycler Bio-Rad iCycler (Bio-Rad, USA). Thermocycling conditions are shown in Table S1. Negative controls (without DNA) were prepared using the same reaction conditions and primers.

PCR products were checked by electrophoresis on 1% agarose gels (SeaPlaque GTG; Cambrex Corp., East Rutherford, NJ, USA) at 100 V, followed by 0.10 µg mL-1 ethidium bromide (EtBr; Bio-Rad) staining. PCR products were visualised in the gel by UV light utilising the Molecular Imager Gel Doc XR system (Bio- Rad). A digital gel image was obtained utilising the image analysis software (software BioRad/Quantity One version 4.6.7). The size of the products was estimated by comparison to marker DNA (λ/HinfIII + φx/HaeIII; Finnzymes). The products were purified using the Geneclean Turbo kit (Qbiogene/MP Biomedicals, Solon, OH, USA) and were quantified with a Nanadrop ND-1000 spectrophotometer (Thermo Scientific, Wilmington, DE, USA).

Subsequently, PCR products were purified using the GeneClean® Turbo kit (Qbiogene, MP Biomedicals) prior to sequencing. Sequencing reactions were done using the refined PCR products and the BigDye® terminator v3.1 Cycle Sequencing Kit (Applied Biosystems, Life Technologies). The target sequences were bidirectionally sequenced, and each set of sequencing data was obtained from at least three independent sequencing reactions (Phred ≥ 20). The sequenced fragments were assembled into contigs using the BioEdit Sequence Alignment Editor version 7 [32], and only bases with standard quality were considered.

The partial sequences were compared with the ones available in the NCBI database using BLASTn. The BLAST X tool (blast.ncbi.nlm.nih.gov/Blast.cgi) was used for *mcy G* and *mcy D* genes. The sequences were annotated for the coding regions by the NCBI ORF Finder and the ExPASY proteomics server.

Nucleotide sequence accession numbers.

Sequence data were deposited in the DNA Data Bank of Japan (DDBJ) under the accession numbers …….. and …… for *16S rRNA, mcy*D and *mcy*G (Table S3).

Phylogenetic analysis.

The gene sequences obtained in this study, as well as the best hit sequences (> 94% identity) retrieved from GenBank, were first aligned using MAFFT version 7 (https://mafft.cbrc.jp/alignment/server/) [33] and then maximum likelihood phylogenetic trees were inferred in IQ-Tree (multicore v1.5.5) [34]. The 166 and 64 sequences compared in phylogenetical analysis for 16S rRNA and *mcy* genes, respectively. Optimum models were used as suggested (BIC criterion) after employing model test implemented in IQ-tree (Table S3). Tree robustness was estimated with bootstrap percentages using 100 standard bootstrap and 10,000 ultrafast bootstrap to evaluate branch supports (Guajardo-Leiva *et al.* 2018). FigTree v.1.2.2 was used for tree visualization. *Gloeobacter violaceus* was set as outgroup for both phylogenetic analyses.

16S-23S rRNA ITS region secondary structure analysis.

The Sequence corresponding to the D1-D1’ helix, D2, D3, BOX B, BOX A and D4 regions of the 16S-23S Internal Transcribe Spacer (ITS) of studied strain was characterized according to the [36]. Comparison of the ITS secondary structures of studied strain and the reference strains were generated using the M-fold web server (version 2.3) [37] under ideal conditions of untangled loop fix and the temperature set to default (37°C).

Chemical Analysis

Cyanobacterial cell extracts were analysed by liquid chromatography mass spectrometry (LC-MS) using a Agilent 1100 Series LC/MSD Trap XCT Plus System (Agilent Technologies). Sample compound separation for microcystin quantitation were chromatographed/analysed with a Luna C18(2) reverse phase column (100 Å, 150mm × 2 mm, particle size 5 µm, Phenomenex) and samples for the analysis of other bioactive compounds were separated on a Luna C8(2) reverse phase column (100 Å, 150mm × 2 mm, particle size 5 µm, Phenomenex). The injection volume of each sample was 10 µl. For the quantitation of MC-RR and MC-LR, a calibration curve was created by plotting the chromatographic peak area that corresponds to the ion mass (MH^- 1036 for MC-RR and MH^- 993 for

MC-LR) [38] against known concentrations. The concentrations were derived from prepared MC-RR (Enzo Life Sciences International) and MC-LR standards.

Results

Environmental parameters

Water at the sampling site was pH = 7.1 and nearly warm (23 °C) at the sampling time. Nitrate (mg L^{-1}) and phosphate (mg L^{-1}) concentrations were 0.09 and 0.1, respectively. Dissolved oxygen (ppm) and conductivity (mS/cm) were 12.1±1.61 and 905.8±3.25, respectively.

Morphology and taxonomic identification

A morphological comparison between isolated (*D. alborizicum*) and the other species of *Demonostoc* including type of the genus, represented by the reference strain *D. muscorum* NIVA-CYA 818 [7], is presented in Table 1.

Macroscopically, isolate 1387 grew attached to the wall of a qanat, exhibiting dark green color. Laboratory observations revealed that it was able to grow fast as a gelatinous biomass, dull olive green, forming a wide range of macroscopic colonies on agar plates (Fig. 1, a). Further, cells colour changed from light green to dark green with the growth progression in plates.

Other morphological characteristics were observed as filaments were generally straight, but sometimes could be twisted, bet or sigmoid (Fig. 1, b). Each filament was a thin, colorless, hyaline sheath (Fig. 1, c). The trichomes were very thin and strongly constricted and the cells were spherical until ellipsoidal that could be much longer than wide (Fig. 1, a-c).

Also were presented about spherical to oblong terminal and oblong intercalary heterocytes, sometimes the terminal heterocytes formed two or three in chain (Fig. 1, d). The reproduction was for fragmentation and formed hormogonia (Fig. 1, e).

The akinetes as well were about terminal and intercalary and formed single or in chain (Fig. 1, f).

The morphology of isolate 1387 is consistent with *Desmonostoc*, because its present typical characteristics of the genus, as cells longer than wide and akinetes that form in chains.

The strain 1387 is morphologically distinct from other species of *Demonostoc* in the present of filaments generally straight, thinner trichomes and largest length-width ratio (Table 1), which means that it has the longest cells of all the species of the genus with respect to the width of the trichome. These characteristics could indicate that the strain is a new species.

Life cycle of strain 1387

Trichomes at the onset of incubation, variously-sized Hormogonia (Fig.2, a) tended to prevail (2 to 10 cells). Hormogonial cells were elongated as well as the cells in vegetative filaments, with tapered terminal cells. These characteristic terminal cells eventually differentiate into heterocytes as the filaments return to the vegetative growth state (Fig.2, b, c). After a short growth period (1–2 days), the formation of pre-heterocytes and heterocytes (Fig. 2, d) intercalary took place in long filaments (15 to 35 cells). Vegetative cells are spherical or slightly oblong, in young filaments, with progress of growth, they became oblong and ellipsoidal (Fig.2, a, d). Degenerated vegetative cells, like necridic cells, also appeared as empty cells, which eventually disintegrated or became detached, resulting in filament fragmentation, detached heterocytes as single or attached together as a group were also observed (Fig. 2, e). In some cases, the space of heterocytes and vegetative cells became longer than usual (Fig. 2, b, d, e). Akinetes were found as single and separated from the main filaments, or as a chain at the end or in the middle of filaments adjacent to heterocytes (Fig. 1, f; Fig. 2, f).

Phylogenetic analyses.

A 16S rDNA fragment was sequenced and aligned with other 166 nucleotide sequences of cyanobacteria obtained from GenBank for phylogenetic analysis. The maximum Likelihood (ML) phylogenetic analysis is shown in Fig. 3.

Although the 16S rRNA gene sequence coupled with its 16S–23S rRNA internal transcribed spacer (ITS) secondary structures represent the core of the present manuscript, the *mcyG* and *mcyD* gene sequences were used as additional molecular markers for characterization of *D. alborizicum*. Different genera and families were used in the construction of the phylogenetic tree, as shown in the figure, each genus is placed in a separate cloud with other similar genera. In addition, the genus *Desmonostoc* has been placed in a separate cloud together

with *Nostoc_muscorum*_Ind33, *Nostoc*_sp_PCC_7906, *Desmonostoc_punense*_MCC_2741, *Nostoc_muscorum*_UTAD_N213, *Desmonostoc*_sp_PCC_7422, *Desmonostoc*_sp_SA25, *Desmonostoc_magnisporum*_AR6_PS and *Desmonostoc_alborizicum*. In fact, the studied strain with the strain *Desmonostoc_magnisporum* AR6 PS (MH497066) is in the same branch with phylogenetic similarity 86.5 percent.

A 1263 and 494 bp nucleotide sequence has successfully been amplified and sequenced for the *mcy*D and *mcy*G genes using specific primers (Table S3). The highest *mcy*D and *mcy*G sequences similarity was found to be 100% and 91.9% of identity with *Nostoc*_sp__IO-102-I (AY566857) and *Nostoc*_sp__CENA88 (GQ259210) respectively (Fig. 4). All representatives of *mcy*G and *mcy*D gene sequences are grouped together in the same clade in the phylogenetic tree. To date, there is no record of *mcy*D and *mcy*G sequences from *Desmonostoc* in the database.

According to the phylogenetic tree we have also compared the 16S rRNA and ITS *p*-distances of our strain with related genera namely (*Nostoc_muscorum*_Ind33, *Nostoc*_sp_PCC_7906, *Desmonostoc_punense*_MCC_2741, *Nostoc_muscorum*_UTAD_N213, *Desmonostoc*_sp_PCC_7422, *Desmonostoc*_sp_SA25, *Desmonostoc_magnisporum*_AR6_PS and *Desmonostoc_alborizicum*) and (Desmonostoc_salinum_CCM-UFV059, Desmonostoc_alborizicum, Desmonostoc_sp._111_CR4_BG11B, Desmonostoc_magnisporum_AR6_PS, Desmonostoc_sp._CCIBT_3489, Desmonostoc_sp._111_CR4_BG11N and Desmonostoc_sp._CCIBt3489_clone_53) respectively.

Results showed that *Desmonostoc_alborizicum* shared a 16S rRNA sequence similarity of 97.27% with *Nostoc_muscorum*_Ind33, 97.84% with Nostoc_sp_PCC_7906, 97.7% with Desmonostoc_punense_MCC_2741, 97.85% with Nostoc_muscorum_UTAD_N213, 97.99% with Desmonostoc_sp_PCC_7422, 97.92% with Desmonostoc_sp_SA25 and 97.99% with Desmonostoc_magnisporum_AR6_PS (Table 2). Results showed that *Desmonostoc_alborizicum* shared a ITS sequence similarity of 98.13% with Desmonostoc_salinum_CCM-UFV059, 97.97% with Desmonostoc_sp._111_CR4_BG11B, 98.70% with Desmonostoc_magnisporum_AR6_PS, 96.67% with Desmonostoc_sp._CCIBT_3489, 98.80% with Desmonostoc_sp._111_CR4_BG11N and 96.67% with Desmonostoc_sp._CCIBt3489_clone_53 (Table S4).

16S-23S rRNA ITS secondary structure.

Six reference sequences were used to search for ITS secondary structure. According to Johansen *et al.* [36], nine different areas (*D1-D1' helix, D2, D3*, BOX B, BOX A, D4 and V3 helix) were found in the ITS secondary structure of studied strain. The D1-D1' and Box-B regions of all studied strains were revealed to be very different in terms of length and shape (Fig. 5 and 6; Tables S6, S7 and S8). The D1-D1' region included a terminal bilateral bulge (A), bilateral bulge (B), unilateral bulge (C), and basal clamp (D) (Fig. 5). The lengths of D1-D1' helix varied from 65 nt (*Desmonostoc magnisporum* AR6_PS) to 69 nt (*Desmonostocalborizicum, Desmonostoc* sp. CCIBT 3489 and *Desmonostoc* sp. CCIBt3489 clone 53) (Table S5). The basal stem revealed to be the same for all studied strains (5'- GACCUA – UAGGUC-3'), except for *Desmonostoc* sp. CCIBT 3489 and *Desmonostoc* sp. CCIBt3489 clone 53, which showed a different basal stem (5' – GACCU- AGGUC 3') (Fig. 5).

Box-B was nominated by Terminal Bilateral Bulge (A), Bilateral Bulge (B). Box-B helix was not found for *Desmonostoc magnisporum* AR6_PS and *Desmonostoc* sp. CCIBT 3489. As to the Box-B, lengths varied from 27 nt (*Desmonostoc salinum* CCM-UFV059, *Desmonostoc* sp. 111_CR4_BG11B and *Desmonostoc* sp. 111_CR4_BG11N) to 37 nt (*Desmonostoc* sp. CCIBt3489 clone 53), with studied strain showing a length of 31 nt (Fig. 6). Moreover V3 helix was only found for *Desmonostoc* sp. CCIBt3489 clone 53 and studied strain and was nominated like The D1-D1' region. The V3 helix was similar in terms of length and shape between the studied strain and *Desmonostoc* sp. CCIBt3489 clone 53 (Fig. 7; Tables S7, S8 and S9).

Results of chemical analysis

Chemical analysis revealed the presence of at least four different microcystin (MC) variants (Table S9). The prominent variant in the sample was Microcystin-LR (MC-LR) in its standard as well in one of its demethylated forms ([D-Asp^3] MC-LR). The other main variant was MC-RR (MC-RR) and one of its demethylated derivatives ([D-Asp^3] MC-RR). The latter, however, was only present in trace amounts. The product ion spectra (MS^2), retention times and molecular ion masses of MC-LR (Figure 8) and MC-RR were consistent with those of the measured standards. The MS^2 spectra of the [D-Asp^3] MC-RR and [D-Asp^3] MC-LR were in agreement with fragmentation patterns described by Fujii *et al.* [38].

Discussion

Ecology and morphology of the novel species

Significant advances in systematics of the order Nostocales have recently been reported with description of several new taxa [9, 12, 19, 39-48].

In temperate regions, the reported abundance and diversity of the nostocacean taxa have increased significantly during the recent decades [49]. Particularly, the genus *Desmonostoc* has been found in different European habitats of Czech Republic, Italy and Spain, besides Africa and New Zealand. Some strains grow in association with mosses or as symbionts of cycadean plants and of *Gunnera* sp. [7]. Nevertheless, the genus remains unexplored in many Asian environments [13], but our morphological studies indicated that the strain 1387 belongs to *Demonostoc*. Using a polyphasic approach, we observed that our strain presented unique characteristics for which we described and proposed a novel species of genus*, Desmonostoc alborizicum* sp. nov*.* The new filamentous heterocytous cyanobacterial species, *Desmonostoc alborizicum* strain 1387, was discovered in an Iranian qanat water supply system with environmental conditions for cyanobacteria growth (*i.e.,* 23 °C, pH = 7.1, nitrogen and phosphorus availability) in western Asia, a novel register of the genus in this region.

A morphological comparison between *D. alborizicum* and other strain of *Desmonostoc* revealed that the filaments were generally straight, and the trichomes were thinner than other species of genus, also the vegetative cells had largest length-width ratio, its means that our species had longest cells of all the species of the genus with respect to the width of the trichome. Morphological traits coupled with the 16S rRNA phylogenetic analysis and the 16S-23S internal transcribed spacer (ITS), from which secondary structures are analyzed, have successfully allowed the separation of *Desmonostoc* at the species level [7, 10, 13, 12, 14].

Molecular evaluation

Phylogenetic studies based on the 16S rRNA gene sequence have shown that taxa assigned to *Nostoc* do not form a monophyletic group [19]. Thus, new *Nostoc*–like genera phylogenetically closely related to *Nostoc sensu strictu* have been described: *Mojavia* Řeháková et Johansen [6], *Desmonostoc* Hrouzek et Ventura [7], *Halotia* Genuário et al. [8], *Aliinostoc* Bagchi et al. [9], and *Komarekiella* G.S. Hentschke J.R. Johansen et C.L. Sant'Anna [50]. In the present study, the *Desmonostoc* clade was found to be sufficiently separated from other well-distinguished clades (Hapalosiphonaceae, *Nodularia, Aliinostoc* and *Anabaena*), which harbored undoubtedly *D. alborizicum* based on the 16S rRNA phylogeny (Fig. 3).

The presence of microcystin biosynthesis (*mcy*) gene cluster in *D. alborizicum* was noticed by the sequencing of the *mcy*D and *mcy*G genes prior to phylogenetic assessment (Fig. 4) and was confirmed by chemical analyses. Microcystins are cyclic heptapeptides that are synthesized non-ribosomally by multifunctional enzymes including polypeptide synthetase (PS) and polyketide synthase (PKS) modules [51, 52]. Potentially toxic cyanobacteria possess the microcystin synthetase *(mcy*) gene cluster that are partial or absent in non-toxic strains [53, 54]. Over 200 structural variants of microcystins have been isolated and characterized to date [55, 56]. They are hepatotoxins implicated in human deaths [57], and chronic exposure to the toxin has shown to cause hepatic and colorectal cancers [58-60]. Actually, among the microcystins detected, was the highly toxic variant MC-LR (median lethal dose [LD_{50}] of 50 µg per kg of mice) was found [61]. The other microcystin variants detected were less potent, nonetheless still known to exert significant toxicity: The LD_{50} value of MC-RR accounts for 600 µg kg^{-1}, 250 µg kg^{-1} for [D-Asp3]MC-RR and 160 – 300 µg kg^{-1} for [D-Asp3]MC-LR [61].

Freshwater *Nostoc* species are predominant in toxic or non-toxic blooms of some lakes of Shoormast and Ali-Abad (Mazandaran Province, Iran) in paddy fields [62-64], and known for their potential for microcystin production [65]. To date, this is the first evidence of a potentially microcystin-producing *Desmonostoc* since no record has reported up to now [10].

In addition, the 16S–23S rRNA ITS and its secondary structure folding of *D. alborizicum* differed from previous described species of *Desmonostoc*, indicating that the ITS can be used as an excellent region for description of new species. The dissimilarities found in the D1-D1´ and Box B helixes (Figs. 5 and 6) suggest the novelty of *D. alborizicum* when compared with related morphotypes (*Desmonostoc_salinum*_CCM-UFV059, *Desmonostoc_alborizicum*, *Desmonostoc*_sp._111_CR4_BG11B, *Desmonostoc_magnisporum*_AR6_PS, *Desmonostoc*_sp._CCIBT_3489, *Desmonostoc*_sp._111_CR4_BG11N and *Desmonostoc*_sp._CCIBt3489_clone_53).

The fact that studied strain's ITS regions were very different from the other related taxa here presented, reinforces that we are in the presence of a new strain. Therefore, these data encouraged us to propose *D. alborizicum* sp. nov. as a new *Desmonostoc* species.

Moreover, our strain showed sequence similarity values of <98% with other related taxa, strongly evidencing the presence of a new species. According to the Yarza et al. [66], identities <98.7% are considered strong evidence for considering compared strains to be in different species. This is reinforced by our results regarding the calculated 16S rRNA *p*-distance between studied strain and related species within the *Desmonostoc* genera, which ranged between 97.27% to 97.99%.

Our results expand the knowledge on genetic diversity and ecological distribution of the genus *Desmonostoc* by a polyphasic analysis of *Desmonostoc alborizicum* sp. nov., and shows its occurrence in an unusual microhabitat in a temperate region.

Description and diagnosis for *Desmonostoc alborizicum* sp. nov.

Desmonostoc alborizicum sp. nov. was set under the provisions of the International Code of Nomenclature for algae, fungi and plants [67]. It is included in the family Nostocaceae sensu Komárek *et al.* [4].

***Desmonostoc alborizicum* (Nowruzi *et al.*) sp. nov.**

Description: Thallus gelatinous, dull olive green, adhering to solid surface. Filaments straight, twisted, bent or sigmoid, in diffluent, hyaline common mucilage, and composed of trichomes uniseriate, 2-3.5 µm wide, with thin, colorless, hyaline, individual sheath and strongly constricted cross-walls. Vegetative cells, first spherical or slightly oblong, later oblong to ellipsoidal, olive green, 2.5-8.5 µm long, with 0.7-4.2 µm length-width ratio. Terminal Heterocytes single, two or three in chain, spherical 2.0-2.5 µm in diameter, or oblong 2.5-2.5 µm wide, 4.0-5.5 µm long; intercalary heterocytes oblong, usually were found only long filaments (15 to 35 cells), 2.0-2.5 µm wide, 4.0-6.0 µm long. In some cases, the space of heterocytes and vegetative cells became longer than usual. Akinetes oblong or ellipsoidal, single and separated from main filaments, or as chains at the end or in the middle of filaments, adjacent to heterocytes, 5.0-6.0 µm wide, 7.5-9.0 µm long. Reproduction for fragmentation to produce hormogonia consisted of 2 to 10 cells.

Declarations

Diagnosis: This novel species was defined according to width of the filament, the length-width ratio, the 16S–23S ITS secondary structure folding, phylogenetic position (based on 16S rRNA gene sequence) and ecological traits.

Etymology: (al.bo.ri'zi.cum. N.L. neut. adj.) The epithet '*alborizicum*' (N. L. neut. adj.) refers to Alborz, name of a mountain range in northern Iran.

Type locality: Fresh water of qanat (36°54'41"N; 4°47'25"E), Golestan province, Gorgan city, Iran.

Holotype: Dried sample of *Desmonostoc alborizicum* 1387 preserved in a metabolically inactive state was deposited into ALBORZ herbarium at the Science and Research Branch of the Islamic Azad University, Tehran, Iran.

Reference strain: *Desmonostoc alborizicum* strain 1387.

Living culture: Living cultures of the type strain (*D. alborizicum* strain 1387), from which the holotype was derived, are available in the Cyanobacteria Culture Collection (CCC) at the Science and Research Branch, Islamic Azad University, Tehran, Iran under the accession number CCC 1387.

DNA sequences: OM800960 (16S rRNA and 16S–23S ITS), OM801557 (*mcy*D), and OM801556 (*mcy*G).

Author Contributions

Bahareh Nowruzi: original concept of paper, original draft preparation, isolation of strain, analysis of molecular data and microscope observation, construction of phylogenetic trees and ITS structures; Itzel Becerra-Absalón original draft preparation, reviewing and editing manuscript.

Conflict of Interest

The authors declare that there are no conflicts of interest.

Funding information

This work received no specific grant from any funding agency

Acknowledgments

We thank Karina Osorio Santos for helping in the elaboration of the life cycle figure and Ricardo García Sandoval for technical assistance in image edition to the figures.

References

1. Price GD, Badger MR, Woodger FJ, Long BM Advances in understanding the cyanobacterial CO2-concentrating-mechanism (CCM): functional components, Ci transporters, diversity, genetic regulation and prospects for engineering into plants. Journal of experimental botany. 2008 May 1;59(7):1441-61. DOI: 10.1093/jxb/erm112
2. Nowruzi B, Haghighat S, Fahimi H, Mohammadi (2018) *Nostoc* cyanobacteria species: A new and rich source of novel bioactive compounds with pharmaceutical potential. J Pharm Health Serv Res 9(1):5–12. DOI: 10.1111/jphs.12202
3. Liu L, Jokela J, Wahlsten M, Nowruzi B, Permi P, Zhang YZ, Xhaard H, Fewer DP, Sivonen K (2014) Nostosins, trypsin inhibitors isolated from the terrestrial cyanobacterium *Nostoc* sp. strain FSN. J Nat Prod 77(8):1784–1790. https://doi.org/10.1021/np500106w
4. Komárek J, Kaštovský J, Mareš J, Johansen JR (2014) Taxonomic classification of cyanoprokaryotes (cyanobacterial genera) using a polyphasic approach. Preslia 86:295–335
5. Komárek J (2016) A polyphasic approach for the taxonomy of cyanobacteria: principles and applications. Eur J Phycol 51:346–353. https://doi.org/10.1080/09670262.2016.1163738
6. Řehaková K, Johansen JR, Casamatta DA, Xuesong L, Vincent J (2007) Morphological and molecular characterization of selected desert soil cyanobacteria: three species new to science including *Mojavia pulchra* gen. et sp. Nov Phycologia 46:481–502. DOI: 10.2216/06-92.1
7. Hrouzek P, Lukesova A, Mares J, Ventura S (2013) Description of the cyanobacterial genus *Desmonostoc* gen. nov. including *D. muscorum* comb. nov. as a distinct, phylogenetically coherent taxon related to the genus *Nostoc*. *Fottea* 13:201–213. DOI: 10.5507/fot.2013.016
8. Genuário DB, Andreote APD, Vaz M, Fiore MF (2017) Heterocyte-forming cyanobacteria from Brazilian saline–alkaline lakes. Mol Phylogenet Evol 109:105–112. DOI: 10.1016/j.ympev.2016.12.032
9. Bagchi SN, Dubey N, Singh P (2017) Phylogenetically distant clade of *Nostoc*-like taxa with the description of *Aliinostoc* gen. nov. and *Aliinostoc morphoplasticum* sp. nov. Int J Syst Evol MicroBiol 67:3329–3338. DOI 10.1099/ijsem.0.002112
10. Alvarenga LV, Vaz MGMV, Genuário DB, Esteves-Ferreira AA, Almeida AVM, De Castro NV, Lizieri C, Souza JJLL, Schaefer CEGR, Nunes-Nesi A, Araújo WL (2018) Extending the ecological distribution of *Desmonostoc* genus: proposal of *Desmonostoc salinum* sp. nov., a novel Cyanobacteria from a saline-alkaline lake. Int J Syst Evol MicroBiol 68:2770–2782. https://doi.org/10.1099/ijsem.0.002878
11. Miscoe LH, Johansen JR, Vaccarino MA, Pietrasiak N, Sherwood AR (2016) Novel cyanobacteria from caves on Kauai, Hawaii. Gebr Bibl Phycologica 120:75–152
12. Saraf A, Dawda HG, Suradkar A, Behere I, Kotulkar M, Shaikh ZM, Kumat A, Batule P, Mishra D, Singh P (2018) Description of two new species of *Aliinostoc* and one new species of *Desmonostoc* from India based on the Polyphasic Approach and reclassification of *Nostoc punensis* to *Desmonostoc punense* comb. nov. FEMS Microbiol Lett 365(24). DOI: 10.1093/femsle/fny272
13. Cai F, Yang Y, Wen Q, Li R (2018) *Desmonostoc danxiaense* sp. nov. (Nostocales, Cyanobacteria) from Danxia mountain in China based on polyphasic approach. Phytotaxa 367:233–244. DOI: https://doi.org/10.11646/phytotaxa.367.3.3
14. Kabirnataj S, Nematzadeh GA, Talebi AF, Saraf A, Suradkar A, Tabatabaei M, Singh P (2020) Description of novel species of *Aliinostoc*, *Desikacharya* and *Desmonostoc* using a polyphasic approach. Int J Syst Evol MicroBiol 70(5):3413–3426. DOI 10.1099/ijsem.0.004188
15. Nowruzi B, Soares F (2021) Alborzia kermanshahica gen. nov., sp. nov.(Chroococcales, Cyanobacteria), isolated from paddy fields in Iran. Int J Syst Evol MicroBiol 71(6):004828. https://doi.org/10.1099/ijsem.0.004828
16. Nowruzi B, Shalygin S (2021) Multiple phylogenies reveal a true taxonomic position of Dulcicalothrix alborzica sp. nov.(Nostocales, Cyanobacteria). Fottea 21(2):235–246. DOI: 10.5507/fot.2021.008
17. Genuário DB, Vaz MG, Hentschke GS, Sant'anna CL, Fiore MF (2015) *Halotia* gen. nov., a phylogenetically and physiologically coherent cyanobacterial genus isolated from marine coastal environments. *Journal of Systematic and Evolutionary Microbiology* 65:663–675. https://doi.org/10.1099/ijs.0.070078-0

18. Rigonato J, Gama WA, Alvarenga DO, Branco LH, Brandini FP et al (2016) *Aliterella atlantica* gen. nov., sp. nov., and *Aliterella antarctica* sp. nov., novel members of coccoid Cyanobacteria. J Syst Evolutionary Microbiol 66:2853–2861. doi: 10.1099/ijsem.0.001066
19. Hentschke GS, Johansen JR, Pietrasiak N, Rigonato J, Fiore MF, Sant'Anna CL (2017) *Komarekiella atlantica* gen. et sp. nov. (Nostocaceae, Cyanobacteria): a new subaerial taxon from the Atlantic Rainforest and Kauai. Hawaii Fottea 17(2):78–190. DOI: 10.5507/fot.2017.002
20. Alvarenga DO, Andreote APD, Branco LHZ, Fiore MF (2017) *Kryptousia macronema* gen. nov., sp. nov. and *Kryptousia microlepis* sp. nov., nostocalean cyanobacteria isolated from phyllospheres. J Syst Evolutionary Microbiol 67:3301–3309. https://doi.org/10.1099/ijsem.0.002109
21. Nowruzi B, Porzani SJ (2021) Toxic compounds produced by cyanobacteria belonging to several species of the order Nostocales: A review. J Appl Toxicol 4510–548. DOI: 10.1002/jat.4088
22. Nowruzi B, Lorenzi AS (2021) Characterization of a potentially microcystin-producing Fischerella sp. isolated from Ajigol wetland of Iran. South Afr J Bot 137:423–433. https://doi.org/10.1016/j.sajb.2020.11.013
23. Nowruzi B, Lorenzi AS (2021) Production of the neurotoxin homoanatoxin-a and detection of a biosynthetic gene cluster sequence (anaC) from an Iranian isolate of Anabaena. South Afr J Bot 139:300–305. https://doi.org/10.1016/j.sajb.2021.02.012
24. Sivonen K (2009) Cyanobacterial toxins, In: Schaechter M. Encyclopedia of Microbiology (Third Edition), Academic Press, https://doi.org/10.1016/B978-012373944-5.00005-5
25. McCleskey RB, Nordstrom DK, Ryan JN, Ball JW (2012) A new method of calculating electrical conductivity with applications to natural waters. Geochim Cosmochim Acta 77:369–382. https://doi.org/10.1016/j.gca.2011.10.031
26. Singh SS, Kunui K, Minj RA, Singh P (2014) Diversity and distribution pattern analysis of cyanobacteria isolated from paddy fields of Chhattisgarh, India. J Asia-Pacific Biodivers 7(4):462–470. https://doi.org/10.1016/j.japb.2014.10.009
27. Sa'id MD, Mahmud AM (2013) Spectrophotometric determination of nitrate and phosphate levels in drinking water samples in the vicinity of irrigated farmlands of Kura town, Kano State-Nigeria. ChemSearch J 4(1):47–50
28. Rippka R, Deruelles J, Waterbury JB, Herdman M, Stanier RY (1979) Generic Assignments, Strain Histories and Properties of Pure Cultures of Cyanobacteria. J Gen Microbiol 111:1–61. https://doi.org/10.1099/00221287-111-1-1
29. Lepère C, Wilmotte A, Meyer B (2000) Molecular Diversity of Microcystis Strains (Cyanophyceae, Chroococcales) Based on 16S rDNA Sequences. Syst Geogr Plants 70(2):275–283. https://doi.org/10.2307/3668646
30. Nübel U, Garcia-Pichel F, Muyzer G (1997) PCR primers to amplify 16S rRNA genes from cyanobacteria. Appl Environ Microbiol 63:3327–3332. DOI: 10.1128/aem.63.8.3327-3332.1997
31. Sambrook J, Russell DW, Molecular Cloning (2001) : A Laboratory Manual. 3rd Edition, Vol. 1, Cold Spring Harbor Laboratory Press, New York
32. Hall TA, BioEdit: (1999) A User-Friendly Biological Sequence Alignment Editor and Analysis Program for Windows 95/98/NT. *Nucleic Acids Symposium Series*, 41: 95–98
33. Katoh K, Standley DM (2013) MAFFT Multiple Sequence Alignment Software Version 7: Improvements in Performance and Usability. Mol Biol Evol 30:772–780. http://dx.doi.org/10.1093/molbev/mst010
34. Nguyen LT, Schmidt HA, von Haeseler A, Minh BQ (2015) IQ-TREE: a fast and effective stochastic algorithm for estimating maximum-likelihood phylogenies. Mol Biol Evol 32(1):268–274. doi: 10.1093/molbev/msu300
35. Guajardo-Leiva S, Pedrós-Alió C, Salgado O, Pinto F, Díez B (2018) Active Crossfire Between Cyanobacteria and Cyanophages in Phototrophic Mat Communities Within Hot Springs. Front Microbiol 9:2039. doi: 10.3389/fmicb.2018.02039
36. Johansen JR, Kovacik L, Casamatta DA, Iková KF, Kaštovský J (2011) Utility of 16S-23S ITS sequence and secondary structure for recognition of intrageneric and intergeneric limits within cyanobacterial taxa: Leptolyngbya corticola sp. nov. (Pseudanabaenaceae, Cyanobacteria). Nova Hedwigia 92(3–4):283–302. DOI: 10.1127/0029-5035/2011/0092-0283
37. Zuker M (2003) Mfold web server for nucleic acid folding and hybridization prediction. Nucleic Acids Res 31:3406–3415. DOI: 10.1093/nar/gkg595
38. Fujii N, Sakaue H, Sasaki H, Fujii N A rapid, comprehensive liquid chromatography-mass spectrometry (LC-MS)-based survey of the Asp isomers in crystallins from human cataract lenses.Journal of Biological Chemistry. 2012 Nov16;287(47):39992–40002. DOI: 10.1074/jbc.M112.399972
39. Han D, Fan EY, Hu EZ (2009) An evaluation of four phylogenetic markers in *Nostoc*: Implications for cyanobacterial phylogenetic studies at the intrageneric level. Curr Microbiol 58:170–176. DOI: 10.1007/s00284-008-9302-x

40. Zapomělová E, Řeháková K, Jezberová J, Komárková J (2010) Polyphasic characterization of eight planktonic *Anabaena* strains (Cyanobacteria) with reference to the variability of *Anabaena* populations observed in the field. Hydrobiologia 639:99–113 https://doi.org/10.1007/s10750-009-0028-y
41. Galhano V (2011) Morphological, biochemical and molecular characterization of *Anabaena*, *Aphanizomenon* and *Nostoc strains* (Cyanobacteria, Nostocales) isolated from Portuguese freshwater habitats. Hydrobiologia 663:187–203. https://doi.org/10.1007/s10750-010-0572-5. Figueiredo D, Alves A, Correia A, Pereira M, Gomes-Laranjo J, Peixoto F.
42. Werner VR, Laughinghouse IVHD, Fiore MF, Sant'Anna CL, Hoff C, de Souza Santos KR, Neuhaus EB, Molica RJ, Honda RY, Echenique RO (2012) Morphological and molecular studies of Sphaerospermopsis torques-reginae (Cyanobacteria, Nostocales) from South American water blooms. Phycologia. Mar 1;51(2):228 – 38. https://doi.org/10.2216/11-32.1
43. Krienitz L, Dadheech PK, Kotut K (2013) Mass developments of the cyanobacteria *Anabaenopsis* and *Cyanospira* (Nostocales) in the soda lakes of Kenya: ecological and systematic implications. Hydrobiologia 703:79–93. https://doi.org/10.1007/s10750-012-1346-z
44. Mishra S, Bhargava P, Adhikary SP, Pradeep A, Rai LC (2015) Weighted morphology: a new approach towards phylogenetic assessment of Nostocales (Cyanobacteria). Protoplasma 252:145–163. DOI: 10.1007/s00709-014-0629-9
45. Singh P, Shaikh ZM, Gaysina LA, Suradkar A, Samanta U (2016) New species of *Nostoc* (cyanobacteria) isolated from Pune, India, using morphological, ecological and molecular attributes. Plant Syst Evol 302(10):1381–1394. https://doi.org/10.1007/s00606-016-1337-z
46. Singh P, Minj RA, Kunui K, Shaikh ZM, Suradkar A, Shouche YS, Mishra AK, Singh SS A new species of *Scytonema* isolated from Bilaspur, Chhattisgarh, India.Journal of Systematics and evolution2016, 54(5):519–527. https://doi.org/10.1111/jse.12202
47. González-Resendiz L, Johansen JR, Escobar-Sánchez V, Segal-Kischinevzky C, Jiménez-García LF, León-Tejera H (2018) Two new species of *Phyllonema* (Rivulariaceae, Cyanobacteria) with an emendation of the genus. J Phycol 54(5):638–652. https://doi.org/10.1111/jpy.12769
48. Saraf AG, Dawda HG, Singh P (2018) *Desikacharya* gen. nov., a phylogenetically distinct genus of Cyanobacteria along with the description of two new species, *Desikacharya nostocoides* sp. nov. and *Desikacharya soli* sp. nov., and reclassification of *Nostoc thermotolerans* to *Desikacharya thermotolerans* comb. nov. *International Journal of Systematic and Evolutionary Microbiology* 69(2):307–315. DOI: 10.1099/ijsem.0.003093
49. Jöhnka KD, Brüggemann R, Rückerc J, Lutherd B, Simone U, Nixdorfc B, Wiednera C (2011) Modelling life cycle and population dynamics of Nostocales (cyanobacteria). Environ Model Softw 26(5):669–677
50. Hentschke GS, Johansen JR, Pietrasiak N, Fiore MD, Rigonato J, Sant'Anna CL, Komarek J Phylogenetic placement of Dapisostemon gen. nov. and Streptostemon, two tropical heterocytous genera (Cyanobacteria). Phytotaxa. 2016 Jan 25;245(2):129 – 43. http://dx.doi.org/10.11646/phytotaxa.245.2.4 129
51. Nishizawa T, Asayama M, Fujii K, Harada K, Shirai M (1999) Genetic analysis of the peptide synthetase genes for a cyclic heptapeptide microcystin in *Microcystis* spp. J BioChem 126:520–529. DOI: 10.1093/oxfordjournals.jbchem.a022481
52. Tillett D, Dittman E, Erhard M, Von Döhren H, Börner T, Neilan BA (2000) Structural organization of microcystin biosynthesis in *Microcystis aeruginosa* PCC7806: an integrated peptide-polyketide synthetase system. Chem Biology 7:753–764. https://doi.org/10.1016/S1074-5521(00)00021-1
53. Kurmayer R, Christiansen G, Fastner J, Börner T (2004) Abundance of active and inactive microcystin genotypes in populations of the toxic cyanobacterium *Planktothrix* spp. Environ Microbiol 6:831–841. DOI: 10.1111/j.1462-2920.2004.00626.x
54. Christiansen G, Molitor C, Philmus B, Kurmayer R (2008) Nontoxic *s*trains of cyanobacteria are the result of major gene deletion events induced by a transposable element. Mol Biol Evol 25:1695–1704. DOI: 10.1093/molbev/msn120
55. Metcalf JS, Codd GA (2014) Cyanobacterial toxins (cyanotoxins) in water. In: Foundation for Water Research, Marlow, Bucks, UK
56. Foss AJ, Aubel MT (2015) Using the MMPB technique to confirm microcystin concentrations in water measured by ELISA and HPLC (UV, MS, MS/MS). Toxicon 104:91–101. DOI: 10.1016/j.toxicon.2015.07.332
57. Jochimsen EM, Carmichael WW, An J, Cardo DM, Cookson ST, Holmes CEM et al (1998) Liver failure and death after exposure to microcystins at a hemodialysis center in Brazil. N Engl J Med 338:873–878. DOI: 10.1056/NEJM199803263381304
58. Ueno Y, Nagata S, Tsutsumi T, Hasegawa A, Watanabe MF, Park HD, Chen G-C, Chen G, Yu S-Z (1996) Detection of microcystins, a blue-green algal hepatotoxin, in drinking water sampled in Haimen and Fusui, endemic areas of primary liver cancer in China, by highly sensitive immunoassay. Carcinogenesis 17:1317–1321. DOI: 10.1093/carcin/17.6.1317
59. Zhou L, Yu H, Chen K (2002) Relationship between microcystin in drinking water and colorectal cancer. Biomed Environ Sci 15:166–171

60. Ren Y, Yang M, Chen M, Zhu Q, Zhou L, Qin W, Wang T (2017) Microcystin-LR promotes epithelial-mesenchymal transition in colorectal cancer cells through PI3-K/AKT and SMAD2. Toxicol Lett 265:53–60. DOI: 10.1016/j.toxlet.2016.11.004
61. Sivonen K, Jones G (1999) Cyanobacterial Toxins. In: Chorus I, Bartram J (eds) Toxic Cyanobacteria in Water: A Guide to Their Public Health Consequences, Monitoring, and Management. E & FN Spon, London, pp 41–111
62. Nowruzi B, Khavari-Nejad RA, Sivonen K, Kazemi B, Najafi F, Nejadsattari T 2013 Identification and toxigenic potential of a cyanobacterial strain (*Stigomena* sp.).Progress in Biological Sciences3(1):79–85
63. Nowruzi B, Khavari-Nejad RA, Sivonen K, Kazemi B, Najafi F, Nejadsattari T (2012) Identification and toxigenic potential of a *Nostoc* sp. Algae 27(4):303–313. https://doi.org/10.4490/algae.2012.27.4.303
64. Nowruzi B, Blanco S, Nejadsattari T (2018) Chemical and molecular evidences for the poisoning of a duck by anatoxin-a, nodularin and cryptophycin at the coast of the Shoormast Lake (Mazandaran province, Iran). Int J Algae 20(4):359–376. DOI:10.1615/InterJAlgae.v20.i4.30
65. Nowruzi B, Sarvari G, Blanco S (2020) Applications of cyanobacteria in biomedicine. In: Konur O (ed) The Handbook of Algal Science, Microbiology, Technology, and Medicine, 1st edn. Elsevier, Amsterdam, p 765
66. Yarza P, Yilmaz P, Pruesse E et al (2014) Uniting the classification of cultured and uncultured bacteria and archaea using 16S rRNA gene sequences. Nat Rev Microbiol 12:635–645. https://doi.org/10.1038/nrmicro3330
67. Turland NJ, Wiersema JH, Barrie FR, Greuter W, Hawksworth DL, Herendeen PS, Knapp S, Kusber W-H, Li D-Z, Marhold K, May TW, McNeill J, Monro AM, Prado J, Price MJ, Smith GF (eds) International Code of Nomenclature for algae, fungi, and plants (Shenzhen Code) adopted by the Nineteenth International Botanical Congress Shenzhen, China, July 2017. Regnum Vegetabile 159. Glashütten: Koeltz Botanical Books 2018. DOI: https://doi.org/10.12705/Code.2018
68. Neilan BA, Jacobs D, Del Dot T, Blackall LL, Hawkins PR, Cox PT, Goodman AE (1997) rRNA sequences and evolutionary relationships among toxic and nontoxic cyanobacteria of the genus Microcystis. Int J Syst Bacteriol 47:693–697. https://doi.org/10.1099/00207713-47-3-693
69. Gkelis S, Rajaniemi P, Vardaka E, Moustaka-Gouni M, Lanaras T et al (2005) Limnothrix redekei (Van Goor) Meffert (Cyanobacteria) strains from Lake Kastoria, Greece form a separate phylogenetic group. Microb Ecol 49:176–182. DOI: 10.1007/s00248-003-2030-7
70. Rantala A, Fewer DP, Hisbergues M, Rouhiainen L, Vaitomaa J et al (2004) Phylogenetic evidence for the early evolution of microcystin synthesis. Proc Natl Acad Sci USA 101:568–573. DOI: 10.1073/pnas.0304489101
71. Fewer DP, Rouhiainen L, Jokela J, Wahlsten M, Laakso K, Wang H, Sivonen K (2007) Recurrent adenylation domain replacement in the microcystin synthetase gene cluster. BMC Evol Biol 7:183. DOI: 10.1186/1471-2148-7-183
72. Rajaniemi P, Hrouzek P, Kastovska K, Willame R, Rantala A, Hoffmann L, Komarek J, Sivonen K (2005) Phylogenetic and morphological evaluation of the genera Anabaena, Aphanizomenon, Trichormus and Nostoc (Nostocales, Cyanobacteria). Int J Syst Evol Microbiol 55:11–26. DOI: 10.1099/ijs.0.63276-0
73. Edwards U, Rogall T, Blöcker H, Emde M, Böttger EC (1989) Isolation and direct complete nucleotide determination of entire genes. Characterization of a gene coding for 16S ribosomal RNA. Nucleic Acids Res 17:7843–7853. doi: 10.1093/nar/17.19.7843

Tables

Table 1

Comparison of morphological features between *Desmonostoc alborizicum* 1387 (In bold) and other species of genus. The information about the other species was obtained from Hrouzek et al. [7], Miscoe et al. [11], Saraf et al. [12], Karbirnataj et al. [14], Singh et al. [45].

	D. muscorum	*D. geniculatum*	*D. vinosum*	*D. magnisporum*	*D. persicum*	*D. punense*	*D. arborizicum* **Strain 1387**
Thallus morphology	± hemispherical colonies, later mucilaginous, amorphous mats	Small, densely clumped colonies	Mucilaginous, sphere colonies	Macroscopic, amorphous colonies	Macroscopic, amorphous, growth	Macroscopic, soft-textured mat-like	Gelatinous mats
Thallus color c	Blue-green, later yellow-brown to olive-green	Purplish black	Gold yellow to light orange	Greenish to dull green, in culture light bluish	Bluish green	Bluish green to dark bluish green	Dark green, Dull olive green
Filaments	Densely entangled, long, irregularly flexuous	Strongly contorted	Twisted and coiled aggregates	Not very long	Long with slight tendency of coiling	Loosely entangled, long	Straight, twisted, bent or sigmoid
Sheath	Distinct at the margin, colorless to yellow-brown	-	Soft diffluent common mucilage. Colorless, without a firm outer layer in filaments	Thin, transparent, hyaline all cross the filament with the visibility at the ends	Light, colored common mucilage, and light mucilaginous envelope all cross the trichome	Distinct, colorless, appearing all throughout the filament	Diffluent, hyaline, common mucilage. Thin, colorless, hyaline, individual envelopment in filaments
Trichomes width (µm)	4.0-6.8	3–8	2.5–3.6	4.1–4.7	2.2–5.4	3.1–4.9	2-3.5
Cross-walls	-	Strongly constricted	Not deeply constricted	Prominently constricted	-	Constricted	Strongly constricted
Cells shape	Shortly barrel to cylindrical, shorter than wide up to isodiametric	Spherical, compressed globose or irregular obovoid	Compressed globose to longer than broad	Barrel to isodiametric	Barrel to cylindrical	Barrel	First spherical or slightly oblong, later oblong to ellipsoidal
Vegetative Cells length / length-width ratio (µm)	3–5(6.5) / 0.4–1.6	2.5-8 / 0.3–2.6	2–4 / 0.5–1.6	4-4.5 / 0.85–1.1	1.9–5.5 / 0.35–2.5	3.5–4.5 / 0.7–1.45	2.5–8.5 / 0.7–4.2
Heterocytes shape	Almost spherical or barrel	Clear, apical, elongated, hemispherical	Intercalary, spherical to compressed	Both intercalary and terminal spherical to oblong	Intercalary almost spherical Terminal oblong and elongated	Both intercalary and terminal spherical to sudspherical	Terminal single, two or three in chain, spherical or oblong ; intercalary oblong
Heterocytes length x width (µm)	(4)6-7.9 x 4.5–6.3(7)	2.7–5.8 x 3.6–6.1	2.5–3.5 x 2.3-3	5.3-6x4.8-5.6	4.6–7.1 x 4.5–7.1	4.7-5.5x3.7-5.1	2–6 x 2-2.5
Hormogonia		Present	Present	Present	Present	Present but rare	Present

	D. muscorum	*D. geniculatum*	*D. vinosum*	*D. magnisporum*	*D. persicum*	*D. punense*	*D. arborizicum* Strain 1387
Akinetes morphology	Long chains, oval shape, with smooth, colorless, yellow cell wall	Intercalary, apoheterocytic, in long series; smooth thickened, wall	Blackish green to yellowish brown, becoming wine-colored	Both terminal and intercalary, large size with irregular shape	Large, solitary, intercalary with barrel shape	In chains, oblong, longer than width, rare	Single or chain at terminal or intercalary, oblong to ellipsoidal
Akinetes length x width (μm)	(6.3)8–12 x 4–8	3.3–7.5 x 5.5-7	3-6.7 x 3–7	-	6.3–9.1 x 4.3-7	6.5-8x3.8-4.5	7.5-9 x 5–6
Habitat	Wet meadows and cultivated soil, pH = 5.3–7.1	Wall of cave from Hawaii	Mixed algae on wall of cave from Hawaii	Freshwater, pH 7.3, 32°C and 90 μS.	Paddy fields	Freshwater, in the transient zone between the water and soil	Freshwater, from Iranian qanat water supply system

Table 2
16S rRNA gene sequence similarity matrix of *Desmonostoc alborizicum* 1387 and related taxa.

	D. muscorum Ind33	*D.* sp. PCC7906	*D. punense* MCC2741	*D. muscorum* UTADN213	*D.* sp PCC7422	*D.* sp. SA25	*D. magnisporum* AR6PS
D. muscorum Ind33							
D. sp. PCC7906	99.28						
D. punense MCC2741	99.14	99.85					
D. muscorum UTADN213	98.85	99.56	99.43				
D. sp PCC7422	98.85	99.56	99.42	99.42			
D. sp. SA25	98.78	99.50	99.35	99.35	99.92		
D. magnisporum AR6PS	98.56	99.29	99.13	99.14	99.56	99.49	
D. alborizicum	**97.27**	**97.84**	**97.70**	**97.85**	**97.99**	**97.92**	**97.99**

Figures

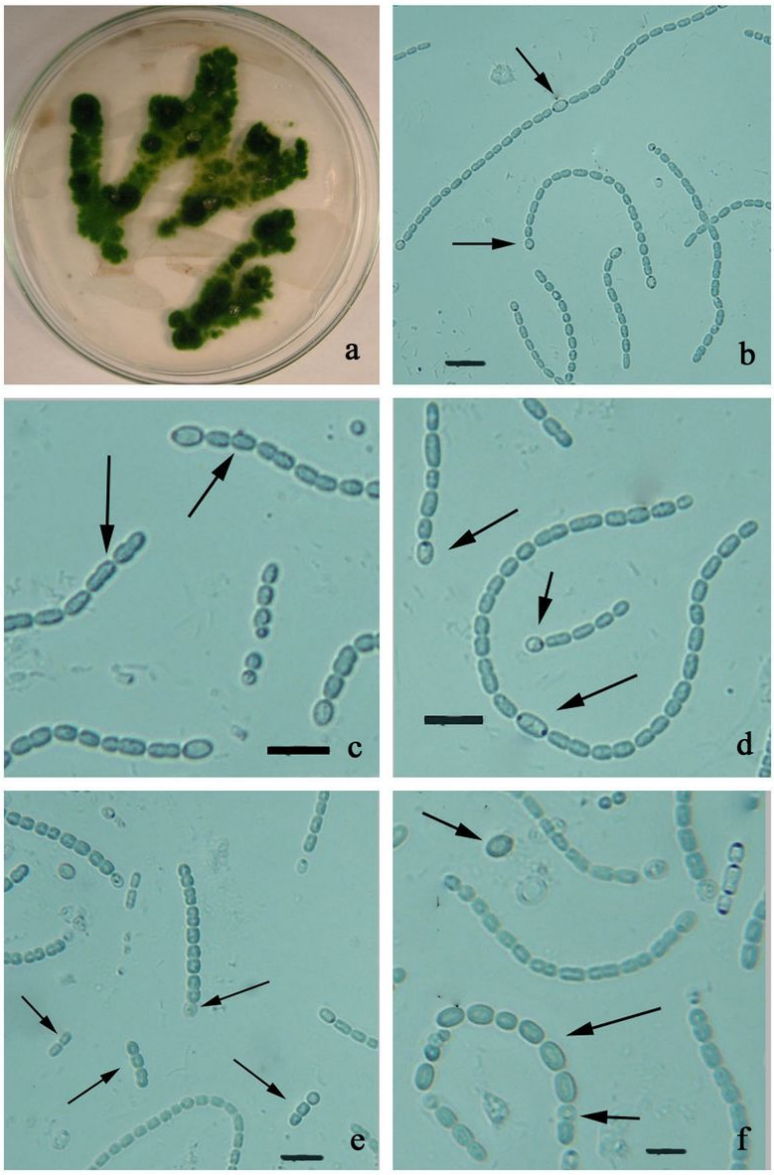

Figure 1

Macroscopic growth and micrographs of *Desmonostoc alborizicum* sp. nov. in culture plate. a) Dark green gelatinous thallus, b) Filaments with intercalary and terminal heterocytes (black arrows), c) Sheath (black arrows), d) Vegetative cells and both intercalary and terminal heterocytes (black arrows), e) Hormogonia (black arrows), sometimes with terminal heterocyte (up central black arrow), f) Akinetes (black arrows), sometimes adjacent to heterocytes (Down black arrow). Scale bar represents 10 ìm.

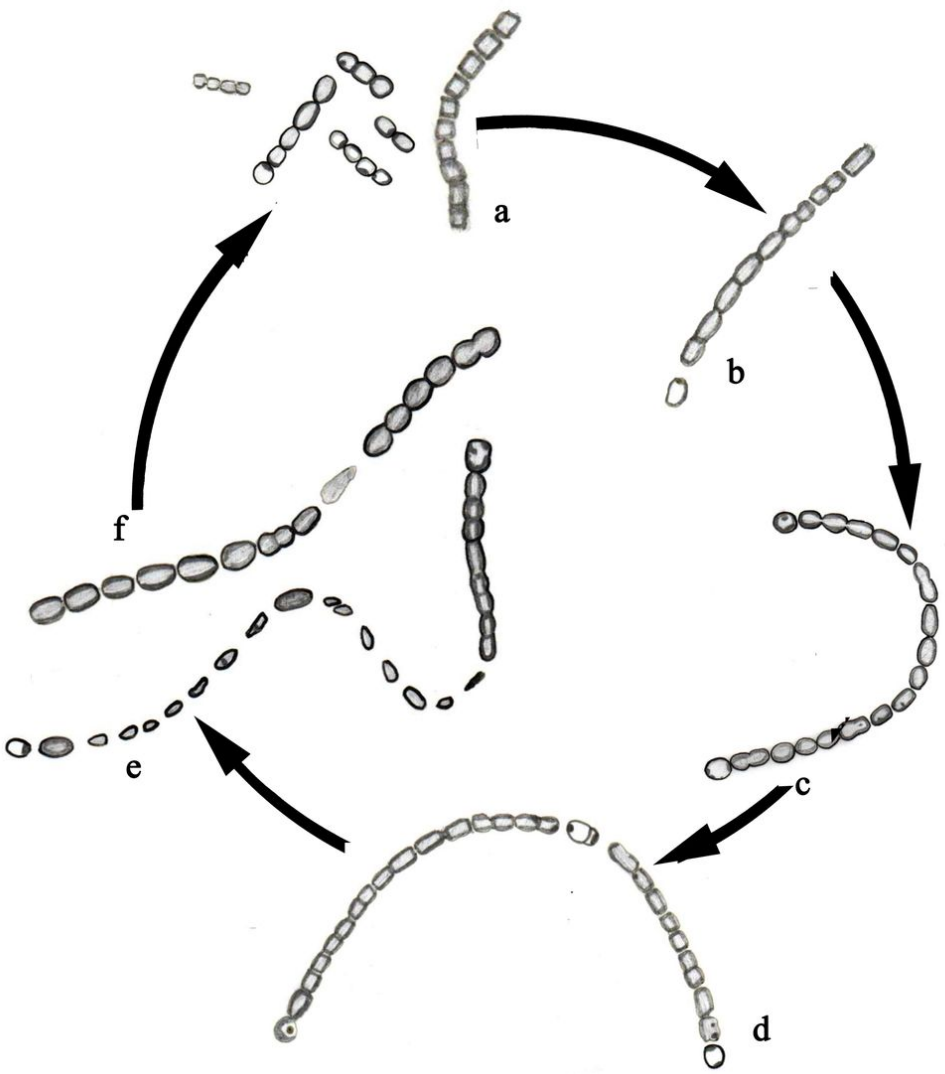

Figure 2

Life cycle of *Desmonostoc alborizicum*: a) Hormogonia, b, c, d) Heterocyte differentiation and vegetative growth of filaments, e) Akinetes formation.

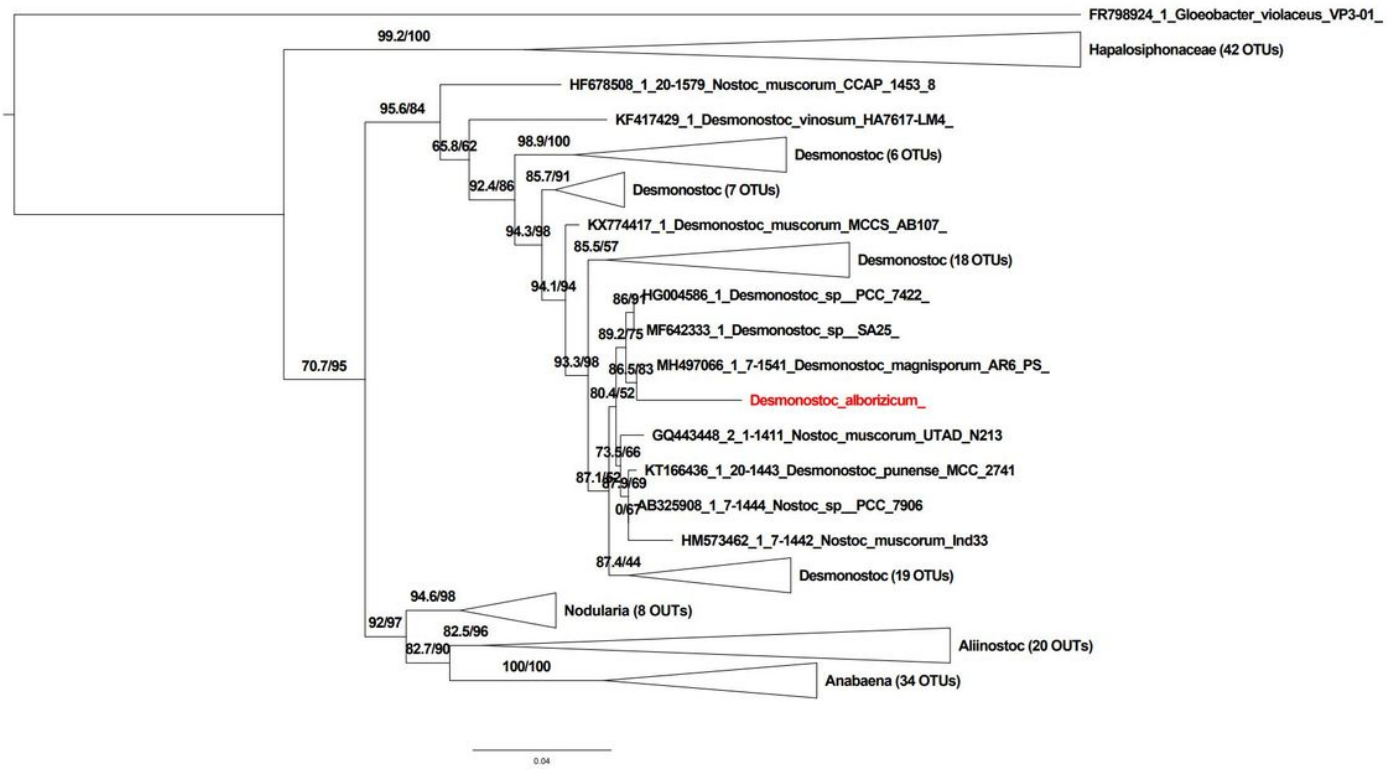

Figure 3

Phylogenetic relationships among *Desmonostoc alborizicum* 1387 (in bold) and related cyanobacteria based on 16S rDNA sequences (2060 bp) with *Gloeobacter violaceus* VP3-01 as outgroup. Numbers near nodes indicate standard bootstrap support (%)/ultrafast bootstrap support (%) for ML analyses.

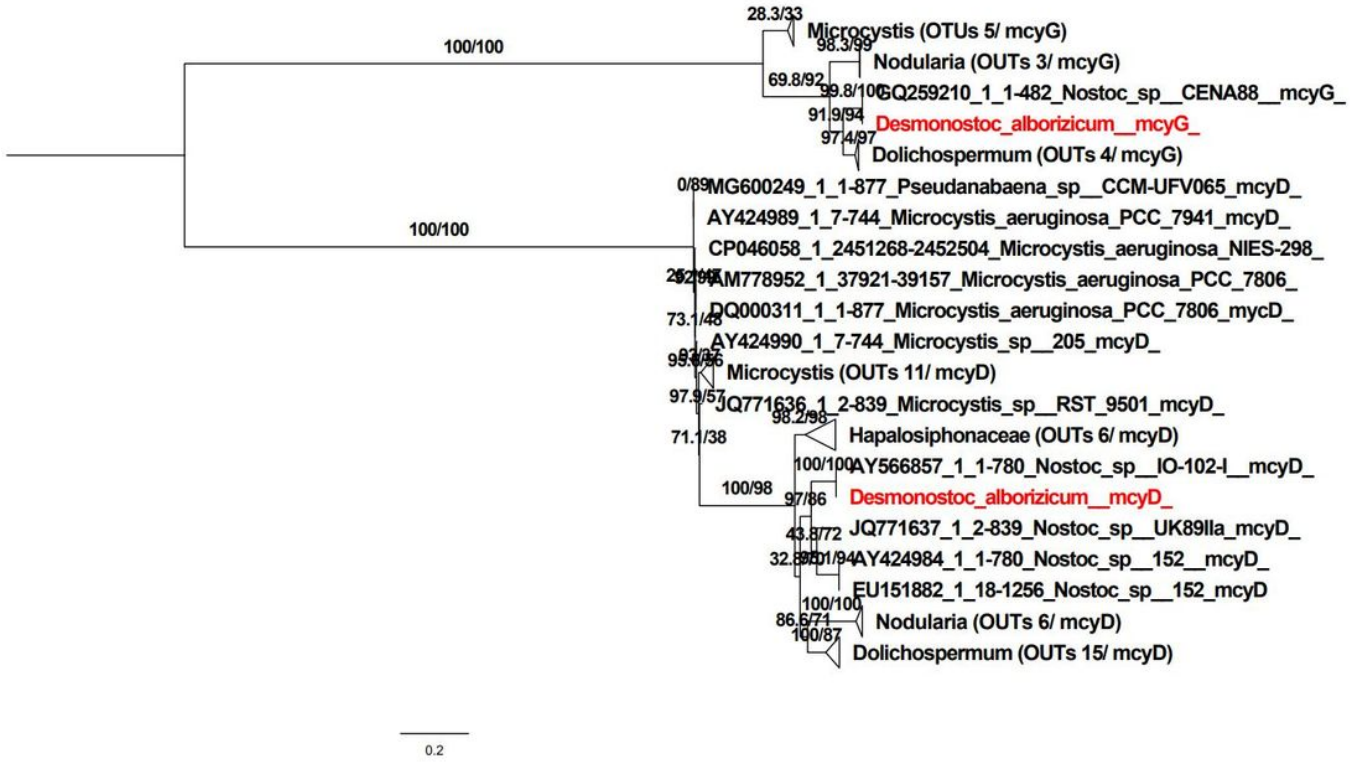

Figure 4

Phylogenetic analyses displaying the relationship among the *mcy*D and *mcy*G genes sequences (1263 and 494 bp). Numbers near nodes indicate standard bootstrap support (%)/ultrafast bootstrap support (%) for ML analyses.

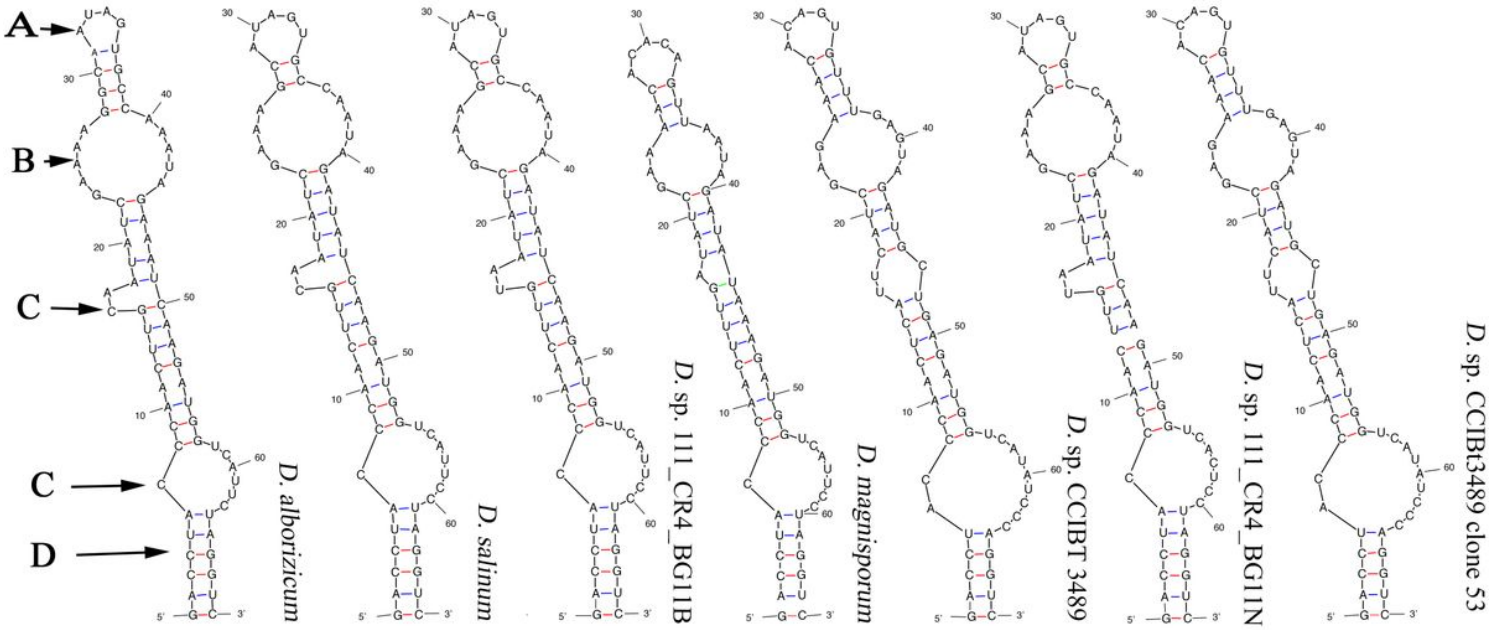

Figure 5

Secondary structures of the D1–D1´ helixes from 16S–23S intergenic spacers.

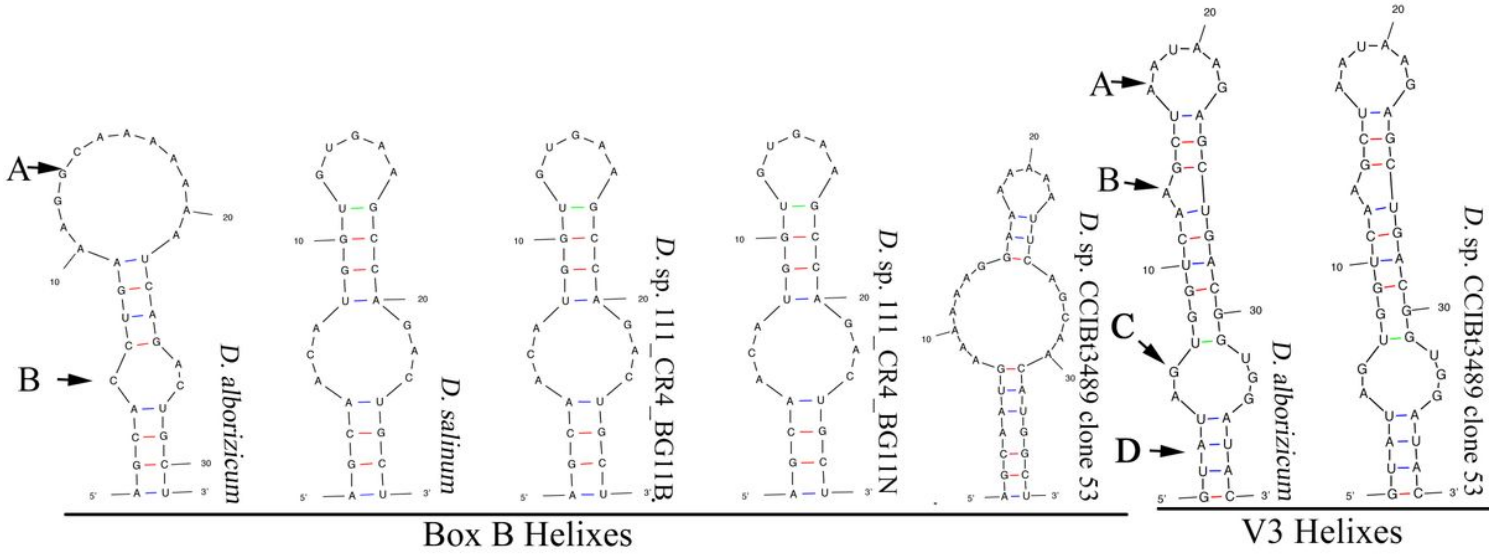

Figure 6

Secondary structure comparisons of the Box B helixes and V3 helixes from 16S–23S intergenic spacers.

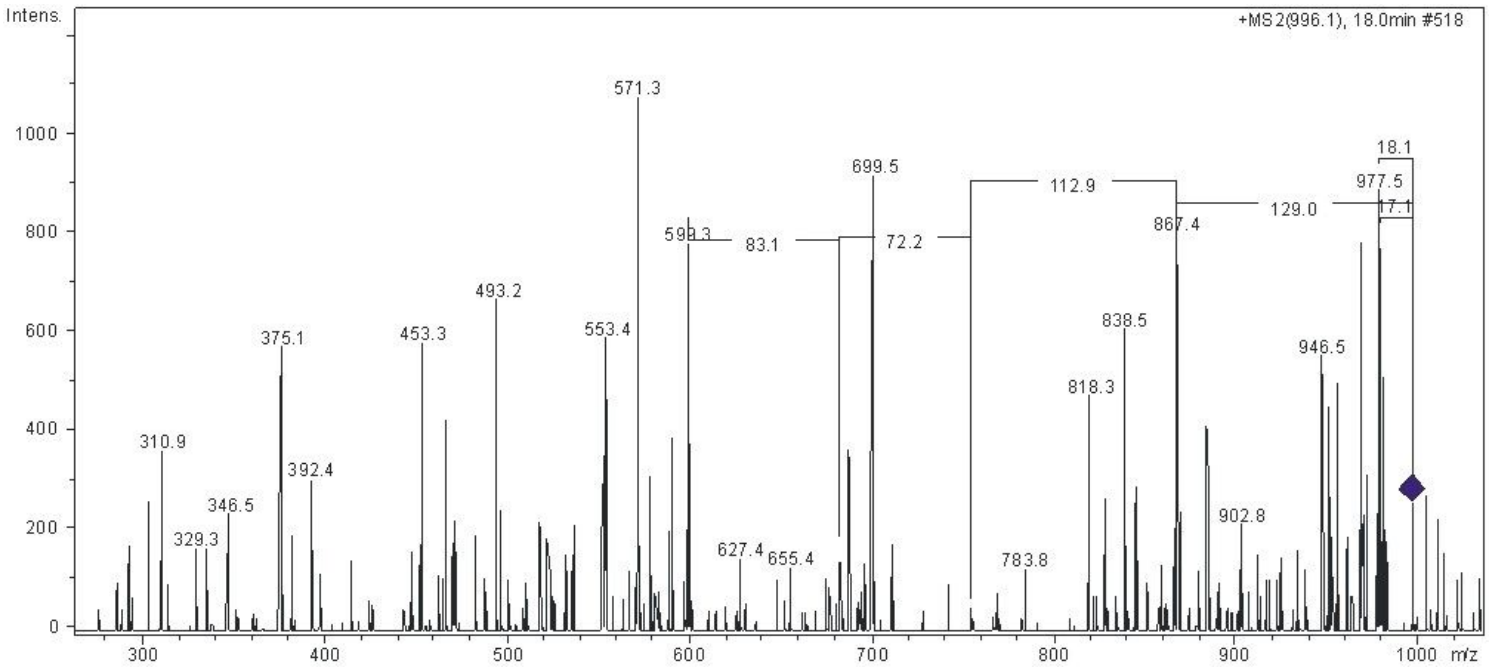

Figure 7

Product ion spectrum of protonated MC-LR (*m/z* 996). Characteristic neutral losses of the parent ion (PI) corresponding to PI - 129 mass units = *m/z* 867 (A), A – 113 mass units (B), B – 72 mass units (C) and C- 83 = *m/z* 599 mass units, are indicated with scale lines.

Supplementary Files

This is a list of supplementary files associated with this preprint. Click to download.

- TableS1S9.docx